IIETA International Information and Engineering Technology Association
Advancing the World of Information and Engineering

Traitement du Signal
Vol. 41, No. 3, June, 2024, pp. 1271-1282
Journal homepage: http://iieta.org/journals/ts

Wayside Condition Monitoring of Metro Wheelsets Using Vibration and Acoustic Sensors

Onur Kilinc[1*], Jakub Vágner[2]

[1] Rail Systems Electrical and Electronics, Motor Vehicles and Transportation Technologies, Vocational School of Transportation, Eskisehir Technical University, Eskisehir 26140, Turkey
[2] Department of Transport Means and Diagnostics, Faculty of Transport Engineering, University of Pardubice, Pardubice 53210, Czechia

Corresponding Author Email: onur_kilinc@eskisehir.edu.tr

https://doi.org/10.18280/ts.410316

Received: 16 October 2023
Revised: 15 February 2024
Accepted: 7 April 2024
Available online: 26 June 2024

Keywords:
wheel defects, wayside diagnosis, speed adaptive fault detection, vibration signals, acoustic signals, wavelet packet energy, time-domain features

ABSTRACT

This paper presents an efficient wayside acoustic and vibration-based detection for wheelset faults on metro trains, which is crucial for the safety of the run. The proposed condition monitoring scheme includes four main steps: data acquisition, signal segmentation by one-period analysis, feature extraction; Time-Domain Features (TDF), Wavelet Packet Energy (WPE) features, and Linear Configuration Pattern Kurtograms (LCP-K), which applies a location invariant textural descriptor to Kurtogram images of the signal, and classification with state-of-art; Fisher's Linear Discriminant Analysis (FLDA), Support Vector Machine (SVM), Decision Tree (Dec. Tree) and Linear Perceptron classifiers alongside classifier combination techniques. During the research, results are obtained on both measured and boosted data. Thus, two databases (A1 and A2), each of which consists of measured vibration and acoustic signals belonging to healthy and faulty cases of the wheelsets of Prague metros, are established. Due to a limited number of faulty instances, features are augmented with Adaptive Synthetic Sampling (ADASYN), and larger vibration and acoustic databases SA1 and SA2 are established to validate methods. Obtained results show that TDF with Dec. Tree classifier can detect wheelset faults by 100% with vibrations signals (A1), and the novel LCP-K algorithm outperforms both acoustic databases (A2 and SA2) up to 93%, and finally, WPE features via combined classifies, reaches a 100% fault detection performance. The proposed framework provides cost-effective maintenance, which can aid metro train specialists, with potential further applicability to other types of railway vehicles.

1. INTRODUCTION

In recent advancements in railway vehicle condition monitoring methods, researchers are focusing extensively on wayside condition monitoring. This involves real-time assessment of sensor data to identify potential mechanical issues with the railway vehicles. The aim is to achieve cost-effective maintenance strategies, which offer greater advantages than periodic servicing or repairs based on condition [1]. Monitoring the condition of the wheelset in railway vehicles is particularly critical for ensuring operational safety. Traditional stationary techniques often require complex static or dynamic laboratory tests and the installation of onboard sensors at specific points on vehicle components. However, wayside condition monitoring offers a more convenient approach for detecting faults in dynamic systems with minimal effort compared to stationary methods. Employing an appropriate evaluation process enables cost-effective maintenance. Additionally, it allows for detecting faults that may gradually or suddenly appear due to significant changes in system parameters, such as the dynamic response of a wheelset, during real-world operations. The scarcity of wheelset fault detection schemes for metro trains in literature, coupled with the limited accuracy observed in existing research compared to our proposed framework, highlights the need for comprehensive understanding and unique approaches to address the metro train and operating company-specific details, underscoring the significance of this research for specialists, especially those in PPTC- Prague Public Transport Company and similar regions across Europe.

Proposed approaches utilizing sensor data from onboard systems have emerged for enhancing running safety monitoring. These techniques require multiple sensor arrays and assessment protocols, along with comprehensive vehicle specifications, to ensure precise condition monitoring [2]. Successful application of these methods demands robust dynamic modelling, effective signal filtration, and addressing calibration challenges.

Fundamental methods for detecting anomalies in railway vehicle operation include utilizing strain, acoustic, accelerometer, or gyroscope sensors [3, 4].

References to wayside condition monitoring systems in Europe are available in the literature [5]. In Czechia, a wayside condition monitoring system called ASDEK enables the measurement of physical parameters such as weight and temperature. This is achieved through sensors installed on or near the railway tracks, catering to train speeds of up to 160km/h at over 40 locations. Real-time detection of wheelset

eccentricity, wheel defects, and hot axle-box/brake disk issues is also feasible, facilitating the implementation of decision-making systems, including railway vehicle stoppage. However, there is currently no available application for metros in the Czechia area.

In the Netherlands, GOTCHA can detect wheel anomalies and offer load measurements with a tolerance of 3% within the operational speed range of 30-70km/h. AVI tags are utilized for vehicle identification. LASCA, on the other hand, utilizes laser beam deflection to detect Q-forces with a 2-3% tolerance at speeds of up to 350km/h, identifying railway vehicles through ZLV bus technology. MULTIRAIL, on the other hand, monitors safety parameters such as wheelset loads and vertical wheel forces, employing RFID for vehicle identification. ARGOS, developed in Austria, employs strain-gauge sensors to monitor axle loads with precision up to 99.5%, offering insights into wheel irregularities at speeds ranging from 10-40km/h. It also assesses wheel roundness with a precision of 0.01mm, utilizing RFID for vehicle recognition. Various other company-specific systems are mentioned in existing literature [6].

The initial adoption of wayside methodologies [7] for identifying wheel anomalies through impact load measurement occurred in New York in 1983. Subsequently, Sweden devised a technique employing strain gauges to detect wheel problems, establishing wayside condition monitoring systems in over 190 locations.

With new advancements, various devices are employed to identify wheel irregularities such as out-of-roundness, shelling, and wheel flats. Strain gauge measurement techniques commonly utilize vertical force and maximum quantities for detecting wheel defects [7]. Utilizing a total of 128 strain gauges enables the identification of such defects for wheels of varying sizes [8].

Observing variations in the refractive index of ultraviolet rays, fiber-optic sensors offer diagnostic capabilities that outperform strain gauge measurements. They exhibit superior resistance to electromagnetic interference and allow fewer challenges in fabrication, recalibration, and installation. Additionally, they are immune to temperature fluctuations, give faster response times, and ensure reliability [9]. Employing fiber-optic sensors enables the detection of rail shear strain, facilitating the identification of vertical impact force. Reports indicate that in addition to axle counting, weight monitoring, and wheel imperfection detection [10] are possible. Literature already presents various other wayside implementations of fiber-optic technologies [11-13].

Utilizing lasers and high-speed cameras offers an alternative method for monitoring wheelset condition and capturing images of wheel profiles. By comparing these images with standard profiles, prognostic wear monitoring is attained [14-16].

The literature also discusses the use of ultrasonic sensors [17-19], employing pulse-echo transmission for detecting wheel defects such as wheel cracks [20]. However, these sensors typically require complex infrastructures and operate at consistent, slow speeds.

Acoustic sensor technology offers a viable approach for monitoring conditions under varying speeds [21-24], particularly focusing on the wheelset. This is because abnormal structures on the wheelset generate a periodic acoustic impulse corresponding to train velocity. Various methods have been explored, including time-domain and frequency energy statistics [25], implementing low-pass filtering and root mean square analysis within suitable time frames, followed by Fourier transform [26]. However, these methods are less effective than vibration signals [27]. Nonetheless, the effectiveness of acoustic wayside applications is reportedly compromised when employing Doppler correction before STFT-Short Time Fourier Transform variants [28].

Vibration sensors provide another efficient means for diagnosing wheel defects. They can effectively detect wheel flats and corrugation, even in noisy signals, through analyzing power cepstrum and comparing energy levels [29]. However, a notable limitation of this approach is the necessity for a constant speed. Additionally, fuzzy logic methods can be employed to monitor the severity of failure on the wheel [30]. In this approach, sensors for detecting vibrations are positioned at the base of the rail, where they assess the centre frequency, train speed, and vibration magnitude. Accordingly, findings suggest that the central frequency and train velocity are the most critical factors affecting output signals. An additional study [31] discusses the efficiency of wavelet-based techniques and direct thresholding in effectively determining the extent of wheel damage when utilizing piezoelectric accelerometer sensors. While employing shear bridges, which include multiple strain gauges, is said to yield superior results compared to accelerometers [32], establishing such trackside systems is challenging due to calibration complexity and cost considerations.

It is essential to select the most appropriate approach for vibration-based condition monitoring of a railway vehicle within its unique wayside setting. Vibration signals typically exhibit non-stationary random characteristics [33]. An efficient method for processing non-stationary signals is STFT, which employs overlapping time windows. However, it requires repeating experiments for consistent performance. Similarly, CWT-Continuous Wavelet Transform) offers fast and convenient non-stationary signal processing. [34], PCA-Principal Component Analysis is utilized to identify frequency differences in the faulty signal despite its unreliability [35].

In contrast to traditional methods, alternative techniques such as AR-Auto-Regressive model [35, 36], ARMA-Auto-regressive Moving Average [37], and EMD-Empirical Mode Decomposition [38] have demonstrated their effectiveness in diagnosing mechanical faults, particularly in conditions with varying speeds, as documented in the literature. Various methods have been proposed, including time-domain statistical features like kurtosis, crest factor [39], variance, skewness, kurtosis, higher-order moments [40], impulse and clearance factors [41], DWT-Discrete Wavelet Transform for denoising, TSA-Time-synchronous Averaging, [42], Kurtograms and wavelets [43, 44], MCKD-Maximum Correlated Kurtosis Deconvolution [45], Gabor wavelets and, wavelet transform [46], HHT-Hilbert Huang Transform and SVMs-Support Vector Machines [47], time domain analysis combined with fuzzy C-means [48], envelope analysis from the Kurtogram [49] as well as various statistical features [50], have been proposed in the literature for detecting rotating component faults. Moreover, recent advancements in deep learning techniques such as LSTM (Long Short Time Memory), RNN (Recurrent Neural Networks), DBN (Deep Belief Network) [51], Multi-Layer Perceptron (MLP) [52], and CNN-Convolutional Neural Networks [53] are also examined in vibration based condition monitoring.

Various techniques discussed in the introduction part require complex mathematical models or sensor calibrations,

which gradually can decrease performance, and specialized personal periodic checks, which make it much more costly (on device measurements) or suffer from low performance in detection (other data-driven methods) and lack of availability to train networks (deep neural networks) and none of them provide a straightforward speed adaptive and short length features via both vibration and acoustic signals with reliability in boosting as ADASYN offers.

This study introduces advanced model-based techniques combined with cutting-edge feature extraction and classification methods to develop an effective framework for monitoring wheelset-related faults. The proposed methods combine one-period signal segmentation, which ensures one rotation of the wheelset under speed-varying conditions, with feature extraction algorithms (TDF, WPE, and LCP-K). These algorithms provide representative features with a fixed output size, and they also benefit from classifier combination techniques. According to the obtained results and validation from metro maintenance specialists, the efficiency of various feature extraction techniques, as compared across different scenarios, is demonstrated.

The paper is structured as follows: Firstly, it outlines the wayside measurement system and details the preparation of the acoustic and vibration databases. Secondly, it presents the methods utilized for signal processing, feature extraction, and classification of wheelset-related faults. Thirdly, it provides the experimental study and analysis of results. Finally, the conclusion is given, followed by a distinct highlights section emphasizing our methodology highlights.

2. EXPERIMENTAL SETUP

In this research, a diagnostic measurement system is built inside the Prague Metro tunnel (metro line A) on the wayside to develop an effective framework for diagnosing faults in metro trains.

2.1 Location and description of the wayside measurement system

The development of the wayside measurement system began in 2013, with optimization of its configuration based on ad-hoc measurements conducted between 2013 and 2014. The initial version of the autonomous system underwent testing in 2015, but validated measurements were only obtained much later due to permission and stability issues. The setup comprises a cabinet housing the Measurement System (MS), track sensors including accelerometers (Z1, Z2, Z3, Z4) and microphones (M1, M2), and optical gates (OGA, OGB). On the measuring track, two pairs of mono-axial accelerometers were installed vertically at the base of the rail between sleepers [54] because the dominant vibration is vertical [55], while two microphones were positioned in the centre of the track between rails. The accelerometers and microphones are installed in the same cross-sections as optical gate sensors *OGA* and *OGB* (Figure 1).

Within the MS Cabinet, industrial computer from AXIOMTEK, alongside the NI cDAQ-9234 system, facilitates data collection at a high sampling rate of up to 51.2kHz (satisfies the minimum required 20kHz in acoustic diagnosis [56]) per channel which should cover most of the characteristic frequencies including those associated with worn wheels. The 2.4GHz Wi-Fi connection between the measuring system and trains allows for the identification of each passing train based on MAC address up to 1km distance with an average of 30 seconds before the arrival of the train operating at 80km/h. The system additionally offers remote control and monitoring functionalities, including monitoring cabinet temperature, available disk space, CPU load, power supply status, etc.

Optical gates allow the initialization of the measurement process; however, a pre-trigger function is needed to record the entire passing. They also enable the calculation of speed and acceleration so that speed-adaptive one-period analysis can be used.

The location of the system was determined based on the experience from previous measurements at other sections. The system is designed to detect other rotational problems in gearboxes and traction motors, which are more detectable with positive traction force. To reduce influences, the search for a suitable location must adhere to fundamental criteria: a straight path, positive elevation (ensuring positive traction force), maximum distance from isolated rails (between signalling sections), maximal distance from lateral service tunnels, and minimal distance from the power supply cabinet. After examining various sections, the ultimate location was selected on Prague Metro Line-A between Dejvická and Bořislavka stations (km 15.1). This track segment features a straight track with a 40‰ elevation, ensuring relatively consistent train speeds and positive high traction force.

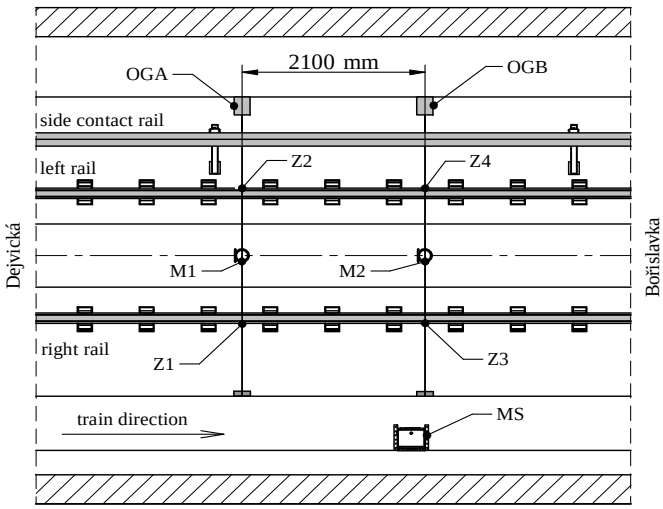

Figure 1. DiMet-autonomous measurement system, configuration inside the tunnel

3. METHODOLOGY

Effective fault characterization is essential for achieving a precise diagnostic mechanism. Whether conducted offline or in real-time, the process of sensor data can indicate potential mechanical faults within the structure, provided that suitable signal processing techniques are applied. This section presents the methodologies dealing with signal processing, feature extraction, and classification employed in this study.

3.1 Fault characteristics of a wheelset

Various potential fault modes for the wheelsets can be characterized based on the mechanical model of the wheelset and its components. Leveraging model-based methodologies

facilitates the estimation of expected fault frequencies associated with the wheelsets of the railway vehicle. Subsequently, these characteristic frequencies can be examined upon using a filtering mechanism prior to subsequent diagnostic procedures.

Two predominant types of faults that can noticeably impact ride quality are wheelset eccentricity (see Figure 2 (a)) and wheel defects (see Figure 2 (b)). Wheel defects, especially those that affect both the rail and vehicle structures, should urgently be identified due to their potential propagation. The characteristic frequency associated with this type of fault is harmonically related to the rotational frequency of the wheelset, and its calculation is shown in Eq. (1).

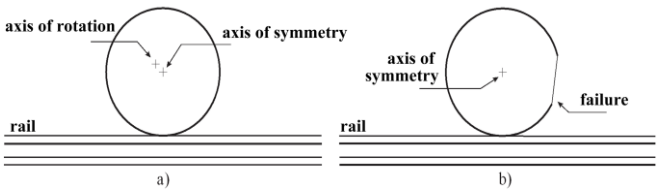

Figure 2. Wheelset-related faults; wheelset eccentricity (a), flat-wheel defect (b)

Eccentric faults in the wheelset imbalance contribute to the wheel rotational frequency in the spectrum. Eq. (1) demonstrates the calculation of this fault frequency, where v represents the translational velocity of the train, and D_k refers to the wheel diameter. Having the possibility to measure the maximum and minimum speed of the train in Dejvická passage, the expected faulty frequency interval can be calculated as in Table 1.

$$f_{ws} = \frac{v}{\pi D_k} \tag{1}$$

Table 1. Wheelset eccentricity (imbalance) fault frequency range for the train set 81-71M

Location	Wheel Diameter [mm]		Speed [m/s]	Frequency [Hz]	
	D_{min}	D_{max}	V_{min}, V_{max}	$f_{ws\,min}$	$f_{ws\,max}$
Dejvická	730	785	15-22.2	6.5-9.7	6.1-9.0

3.2 One-period signal segmentation

This method assumes that vehicle vibrations transmit to the rail on the contact points with the wheel. The wheelset serves as the fundamental unit for diagnosis within the train running gear. By referencing the train identification and maintenance database, one can link the measured wheelset to its identification and maintenance history, as well as that of related components like traction motors, gearboxes, and bearings. The initial step involves segmenting the recorded signals into blocks, each representing a single wheelset rotation, with the block length determined by the wheel diameters and train speed obtained from the maintenance database and optical gate signals, respectively. Eq. (2) shows the calculation of the signal block length:

$$n_i = 2 \cdot \mathrm{round}\left(\frac{\pi \cdot d_i \cdot f_s}{2 \cdot v_i} \right) \tag{2}$$

Assuming that i as the index of wheelset, n_i as the sample count in the block, d_i as the mean diameter of left and right wheels, v_i is the velocity of wheelset, f_s as the sampling frequency. Train speed is calculated by Eq. (3) with a tolerance of 0.5km/h validated through hundreds of passes:

$$v_i = \frac{L \cdot f_s}{s_{Bi} - s_{Ai}} \tag{3}$$

Given L as the distance between optical gate sensors, s_{Ai} as the sample number for detecting the centre of the wheelset number i by optical gate OGA, similarly s_{Bi} is the sample number from optical gate OGB. Centre of the block should be positioned at sample s_{Ai} for segmenting signals from Z1 and Z2 sensors or at sample s_{Bi} in case of segmenting signals from Z3 and Z4 sensors.

Wheelset velocities are retrieved from the train and are fitted by a linear function. A histogram of speed values is given in Figure 3, while Figure 4 shows an example of one period block signal with the following parameters: $v_i = 22\mathrm{m.s^{-1}}$; $d_i = 0.745\mathrm{m}$; train ID: 108, wheelset No: 13, passing ID: 20160713_070409.

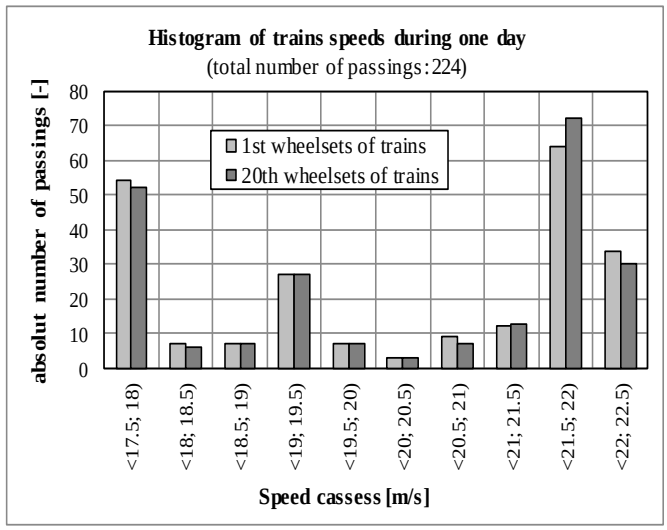

Figure 3. Histogram of train velocity measurement in one day

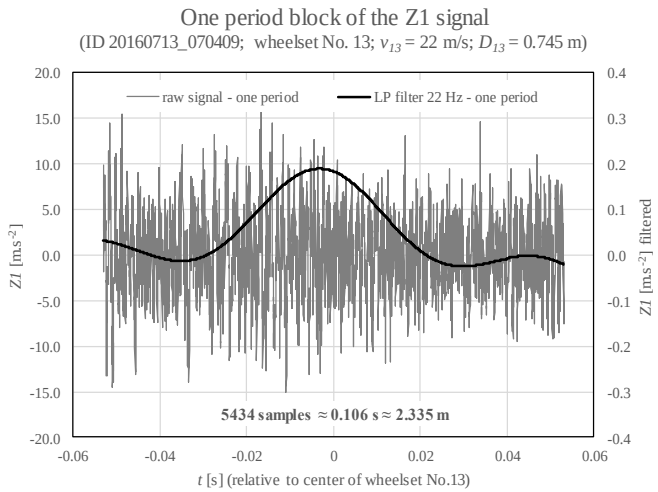

Figure 4. One-period segmented vibration signal

3.3 Wavelet packet analysis

Fault transients can appear randomly, their exact location can be dominated by significant environmental noise, even with a full understanding of the dynamic system model. However, in mechanical fault diagnosis, these transients exhibit periodicity, making frequency domain methods feasible. To investigate such periodic transients, WPT-Wavelet Packet Analysis offers a solution, as in STFT [57], but provides variable frequency resolution, as highlighted in academic literature for time-frequency analysis. Through wavelet packet analysis, the Fourier spectrum can be partitioned into numerous frequency bands, allowing for the desired frequency resolution. WPT shares a structure similar to DWT-Discrete Wavelet Transform, which enables a multi-scale time-frequency representation of signal data [58]. Various wavelet functions such as Haar, Daubechies, and Symlets [59] can be utilized in the calculation of DWT. The mathematical representation of the DWT for a discrete signal $x[n]$ is shown in equations Eq. (4) and Eq. (5) with the wavelet basis function $\psi_{a,b}$ while a is the dilation and b is the location parameter.

$$\psi_{\mathrm{a,b}}[n] = \frac{1}{\sqrt{a}}\psi\left[\frac{n-b}{a}\right] \tag{4}$$

$$\mathrm{X[a,b]} = \sum_{n=-\infty}^{\infty} x[n]\psi_{\mathrm{a,b}}[n] \tag{5}$$

Utilizing filter banks known as QMF-Quadrature Mirror Filters, DWT operates as a multiresolution analysis tool [60], employing both low-pass and high-pass filtering operations. The low-pass filter generates approximation coefficients (A), while the high-pass filter produces detail coefficients (D). This method outperforms STFT in offering improved time resolution at high frequencies while maintaining adequate frequency resolution at lower frequencies. However, DWT suffers from reduced frequency resolution at higher frequencies compared to WPT, which employs linear combinations of wavelet functions and retains the advantages of orthonormality and time-frequency domain localization. If we assume the number of levels n_w; $k_w = 2^{n_w}$ refers to the number of wavelet packets in WPT. The signal is then filtered to capture low and high-frequency components, followed by downsampling for the subsequent level. Figure 5 illustrates a two-level decomposition of the wavelet packet tree for a discrete signal $x[n]$, where $h[n]$ is a low-pass (L) and $g[n]$ is a high-pass (H) QMF results yielding approximation (A) and detail (D) coefficients, respectively.

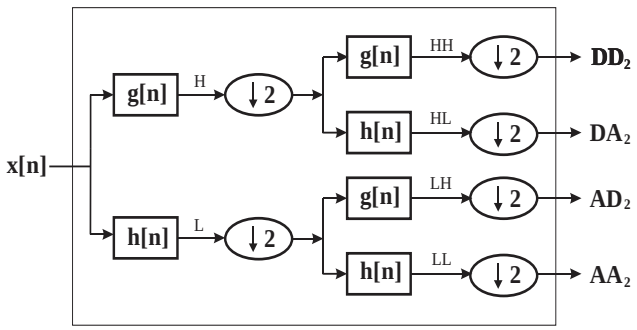

Figure 5. Two-level wavelet packet decomposition

However, the components of WPT remain non-translation invariant, and addressing this issue can be accomplished by computing the energy levels of each wavelet packet k_w as given in Eq. (6) where $c_{j,n}$ denotes the wavelet coefficients at index $j-th$ on n_w-th level. Utilizing these energy measures directly as a feature vector is feasible due to the reduction of feature dimension enabled by WPE [61], ensuring that periodic transients propagate effectively in WPE coefficients [62].

$$E_{n_w,k_w} = \sum_j c^2_{j,n_w,k_w} \tag{6}$$

3.4 Linear configuration pattern Kurtograms

Methods based on spectral kurtosis are widely used in monitoring the condition of rotating machinery to detect signal non-stationarities. Recently, a more efficient approach called Kurtogram has been introduced as a fourth-order analysis tool [63]. In the Kurtogram method, signals are transformed into frequency-delta frequency spectra, allowing for the investigation of transients associated with faulty conditions, which exhibit high kurtosis in a dyad view $(f, \Delta f)$. However, the main drawback of Kurtogram is its computational inefficiency. To address this, a faster algorithm called FK-Fast Kurtogram has been developed, which has a similar complexity to FFT-Fast Fourier Transform [49]. FK divides frequency bands finely and presents the magnitude of each spectral kurtosis in a grid view, represented as a dynamic intensity image [49]. Additionally, LBP-Local Binary Patterns is a popular method in two-dimensional pattern recognition that focuses on texture recognition and bioinformatics [64]. LBP aims to maximize mutual information by comparing pixel intensities in the surrounding area while labelling discriminative features of a two-dimensional signal. For a given circular window radius, it calculates binary patterns for each neighbourhood using a specific formulation as described in the study [65] in Eq. (7):

$$LBP(P,R) = \sum_{i=0}^{P-1} u(g_i - g_c)2^i \tag{7}$$

where, g_i denotes the intensity for i_{th} pixel while g_c refers to the centre pixel intensity, P is the number of pixels at radius R.

Therefore, the LBP method can function effectively across varying colour maps. A recent study [66] introduces an enhanced variant of LBP known as LCP-Local Configuration Pattern, which is capable of identifying similar patterns with differing orientations. This algorithm integrates LBP features with microstructural details of the image, ensuring a consistent output. By combining LCP with the FK method, a novel approach, LCP-K-Linear Configuration Pattern-Kurtograms, is developed, offering robust dimension reduction and accurate representation of fault signatures in any one-dimensional signal.

Initially, the five-level Fast Kurtogram (FK) is computed. Subsequently, the Kurtogram image is resized to 128x128 pixels using bi-cubic interpolation [67] and converted to grayscale.

Lastly, the LCP is applied to the grayscale image, which is partitioned into 16×16 blocks, extracting 81×1 feature vectors of double precision.

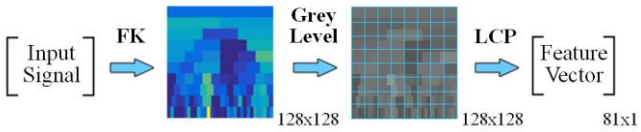

Figure 6. LCP-K Feature extraction scheme for a one-period segmented healthy signal

In conclusion, our LCP-K algorithm (Figure 6) [68] applies a location invariant textural descriptor to Kurtogram images of the signal to discard fluctuation effects in Kurtogram images ensuring the representative output feature vectors with the same size addressing signal sample size issues.

3.5 Time-domain features

In vibration-based analysis, anomaly signals exhibit similar temporal characteristics statistically. Utilizing statistical features in time domain is a fundamental and effective way in feature extraction, in machinery condition monitoring. In this investigation, mean (μ), standard deviation (σ), maximum (max), minimum (min), kurtosis, skewness and crest factor; a measure of RMS-Root Mean Square and energy, are computed, as inspired by studies [48, 50] for mechanical fault detection. The proposed TDF-Time Domain Features are computed via Eqs. (8)-(11) for a given discrete signal x_n with length N, and then concatenated in a matrix of double precision.

$$Energy: \sum_{n=1}^{N} |x_n|^2, \quad Skewness: \sum_{n=1}^{N} \frac{(x_n-\mu)^3}{(N-1)\sigma^3} \tag{8}$$

$$Kurtosis: \sum_{n=1}^{N} \frac{(x_n-\mu)^4}{N\sigma^4} - 3 \tag{9}$$

$$Crest\ Factor: 20\left[\log_{10}\left(\frac{\max(x_n)}{\mathrm{RMS}(x_n)}\right)\right] \tag{10}$$

$$TDF = \begin{bmatrix} energy, mean, std.deviation, max, \\ min, kurtosis, skewness, crest\ factor \end{bmatrix}_{8x1} \tag{11}$$

3.6 Adaptive synthetic sampling

The most common data encountered in wayside railway vehicle fault detection is healthy, leading to the observation of a significantly greater number of normal signal samples than abnormal ones. Moreover, obtaining abnormal samples for vehicles of the same type is costly unless a real-time measurement system is consistently maintained.

Typically, the number of observations (m_o) within each class should exceed the length of each feature vector (n_o), or an insufficient case scenario ($n_o \geq m_o$) arises [69]. This insufficient case is often encountered in applications such as signature and voice recognition due to limited observed samples. Misclassifying faulty samples as healthy (false negatives) can be highly challenging to recover from. In such cases, the minority class, comprising less frequent feature vectors, requires oversampling. A straightforward approach to tackle this issue is to accurately interpolate the minority class samples to generate new samples.

To address imbalanced datasets, the literature suggests using SMOTE-Synthetic Over Sampling Method [70]. This approach involves linearly interpolating existing feature vectors from the minority class to create new vectors. However, SMOTE solely targets the minority class vectors, disregarding the majority class samples, which may not always be a practical method for generating additional data. This issue is addressed by an extension of the SMOTE technique known as ADASYN-Adaptive Synthetic Sampling [71]; ADASYN considers samples across each class boundary and dynamically generates samples for the minority class.

The application of ADASYN for feature generation is illustrated in Figure 7 using our wayside measurement database. Specifically, we demonstrate its utilization for the minority class, which comprises 16 observations associated with wheel faults ($m_0^{Faulty} = 16$) and the majority healthy class with 128 normal observations ($m_0^{Normal} = 128$). The parameters k-ADASYN and k-SMOTE, which are required for density estimation in the k-Nearest Neighbour (kNN) utilizing Euclidean distance, are both set to a default value of 5. ADASYN boosts each specific feature within the minority class by considering both classes, resulting in the creation of a total of m_0^{Normal}-$m_0^{Faulty} = 112$ number of feature vectors that contribute to reinforcing the minority class. It is important to highlight that the synthesized feature vectors gather near the boundaries between classes, and the outlier sample on the right top was not used to generate a new sample by algorithm automatically. This enhances the reliability and complexity of the database, minimizing the impact of outliers rather than solely relying on in-class interpolation.

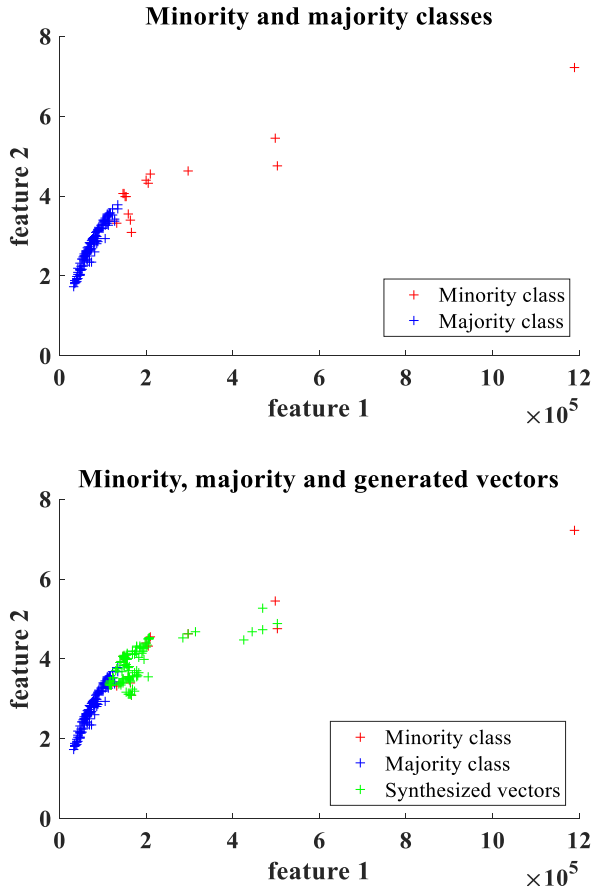

Figure 7. Utilizing ADASYN to generate synthetic samples in the minority class to achieve a balance with the majority class [72]

4. RESULTS AND DISCUSSION

In this section, three primary analyses linked to the detection of faults in metro train wheels have been presented. To do so, advanced feature extraction and classification techniques were applied to our database to assess both acoustic and vibration-based diagnostic methods.

4.1 Acoustic and vibration signal databases

The signal repository comprises original acoustic and vibration signals obtained from the wayside measurement system situated between Dejvická and Bořislavka metro stations. Within this database framework, signal classification is treated as a two-class (normal and defective) challenge. Faulty data was gathered from a wheelset (axle 7 on ID-108 metro train), exhibiting wheel flats on both wheels. In contrast, normal data was retrieved from the remaining wheelsets (axles: 1-4, 11-14) of the same train set, captured during daily operations using Z1-Z2 accelerometers and M1-M2 acoustic sensors. Eight train passages were recorded in total, with the faulty wheelset being inspected in the depot (faulty wheel shown in Figure 8). Detailed database specifications are provided in Table 2.

Before further processing, all signals are segmented according to one-period analysis for each axle.

To construct a robust model, the database is prepared with comprehensive information sourced from metro maintenance records, ensuring a balanced representation of both healthy and faulty conditions. Furthermore, in response to the limited observations of faulty conditions during the eight passing times of the trainset with a defective wheel (ID-108), additional samples are wisely generated by adapting feature vectors from measured vibration (A1) and acoustic (A2) signals using ADASYN. This strategic approach results in the creation of synthetically oversampled databases SA1 and SA2 for vibration and acoustic signals, respectively, thereby facilitating a more comprehensive evaluation of the framework efficiency.

Figure 8. A wheel flat developed at the center of the contact area due to blockage or partial blockage on the seventh wheelset of metro train ID-108

Table 2. Description of vibration and acoustic databases

Measured Faulty Samples	Synth. Faulty Samples	Total Normal Samples	Sensors	Dataset
16	0	16	Z1-Z2	A1
8	0	8	M1-M2	A2
16	112	128	Z1-Z2	SA1
8	56	64	M1-M2	SA2

4.2 Results of vibration-based wheelset condition monitoring

In the proposed method for wayside diagnosis, the fluctuating speed leads to varying sample sizes in the output signals during one-period signal segmentation.

Hence, feature extraction techniques are applied to standardize the outputs and achieve substantial dimension reduction for the classification of normal and faulty instances. This section examines the performance of three feature extraction methodologies; WPE features [62] (32×1) come from five-level wavelet decomposition tree, eleven time-domain statistical features (TDF), and a Kurtogram textural descriptor; LCP-K features (81×1) classified with four cutting-edge classifiers: support vector machine with linear kernel (SVM-I) [73], PERLC-Linear Perceptron [74], FLDA-Fisher's Linear Discriminant Classifier [75] and Dec. Tree-Decision Tree [76]. The assessment of these models is performed either via n-fold cross-validation, which yields the highest classification performance, or splitting the training and testing samples in half for each class and applying classifier combining techniques.

The results presented in bold text in Table 3 indicate that the most effective feature extraction method for the two-class classification of wheel defects in vibration-based diagnosis is TDF. While SVM-I demonstrates superior performance in classifying the synthesized cases (SA1), PERLC performs comparably to SVM-I and outperforms SVM-I in classifying measured-only data (A1). According to the results, wayside diagnosis of wheel defects can be achieved with a 100% success rate without employing any pre-processing when utilizing TDF features with the Dec. Tree classifier.

Further exploration is conducted to assess the performance of various classifier combination techniques, which may yield superior results compared to individual classifiers. Proposed methods with different classifier combining methods are employed with our base classifiers: FLDA, SVM-I, Dec. Tree, and PERLC. Multiple classifier combination techniques are performed, including Prod-C (Product Combiner), Mean-C (Average Combiner), Med-C (Median Combiner), Max-C (Maximum Combiner), Min-C (Minimum Combiner), and Vote-C (Majority Voting) [77]. Each dataset (A1, SA1) is divided equally for each class (normal, faulty) to conduct training and testing stages.

Table 4 and Figure 9 show the recognition rates (ACC) along with ROC-Receiver Operating Characteristic curves, which encompass AUC-Area Under Curve values offering insights into false positive detection rates of wheel defects, both for measured and synthesized data, when employing classifier combination techniques.

Table 3. Wheelset fault detection accuracies for measured and boosted data from Z1-Z2 sensors

Classifier	Classification Performance (%)				
	WPE	TDF	LCP-K	Average	Dataset
FLDA	59.4	93.8	62.5	71.9	A1 (8-fold)
	95.7	99.2	95.5	96.8	SA1 (16-fold)
SVM-I	93.8	93.8	68.8	85,5	A1 (8-fold)
	99.6	**100**	96.9	**98.8**	SA1 (16-fold)
Dec. Tree	90.6	**100**	84.4	91.7	A1 (8-fold)
	98.1	**100**	91.8	96.6	SA1 (16-fold)
PERLC	96.9	93,8	87.5	**92.7**	A1 (8-fold)
	99.2	99.2	**97.7**	**98.7**	SA1 (16-fold)

Table 4. Wheelset fault detection accuracies for measured and boosted data using combined classifiers

Combined Classifier	Classification Performance (%)			Train	Test	Dataset
	WPE	TDF	LCP-K			
Prod-C	68.8	81.3	68.8	16	16	A1
	76.7	92.2	90.6	128	128	SA1
Mean-C	**100**	87.5	81.3	16	16	A1
	73.4	89.1	89.8	128	128	SA1
Med-C	**100**	87.5	81.3	16	16	A1
	70.4	88.3	88.3	128	128	SA1
Max-C	68.8	81.3	62.5	16	16	A1
	82.8	**96.1**	89.8	128	128	SA1
Min-C	68.8	81.3	68.8	16	16	A1
	80.5	**96.1**	89.8	128	128	SA1
Vote-C	**100**	93.8	75.0	16	16	A1
	87.5	88.3	91.4	128	128	SA1

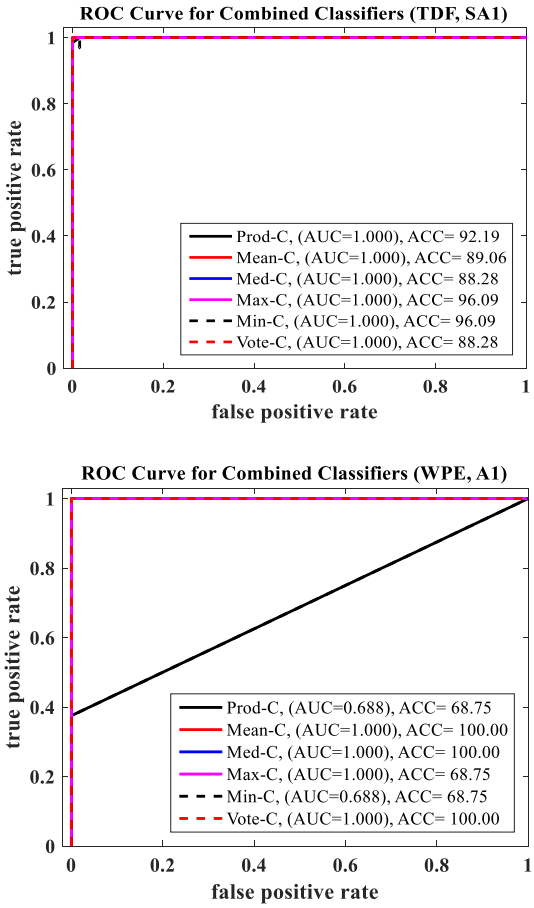

Figure 9. ROC curves (classifier combination techniques) for TDF on dataset SA1 (top), WPE on dataset A1 (bottom)

Obtained results show that, among classifier combination methods like Med-C, Mean-C, and Vote-C, WPE stands out as the only technique capable of classifying measured wheelset faults. However, in the case of synthetically generated databases, TDF remains the top performer with an accuracy of 96.1%, while LCP-K outperforms WPE with a success rate of up to 91.4%.

4.3 Results of acoustic-based wheelset condition monitoring

This section presents acoustic-based condition monitoring results. The same procedure in vibration-based diagnosis is carried out in the feature extraction and classification process (WPE, TDF, and LCP-K techniques with the classifiers FLDA, SVM-I, Dec. Tree, and PERLC). To ensure reliable assessment, a 4-fold cross-validation is conducted for the measured signals database (A2), whereas for the hybrid database (SA2) comprising both measured and synthetically oversampled features, an 8-fold cross-validation is employed. As indicated in Table 5, the LCP-K algorithm, when used with the Dec. Tree classifier, can effectively identify faulty wheelsets with a success rate of 87.5% in the A2 dataset. In the SA2 dataset, its accuracy increases significantly to 93% with the SVM-I classifier. While other feature extraction methods exhibit similar accuracies in either A2 or SA2 datasets, LCP-K stands out as the only method capable of classifying samples in both acoustic-based databases. Note that the utilization of microphone sensors in diagnosis yields notably lower results compared to vibration-based diagnosis, when only measured cases are utilized in the training and testing. However, the inclusion of synthetic feature samples demonstrates a considerable improvement in classification.

To conclude, in acoustic-based condition monitoring, the impact of noise and the Doppler effect is not considered, which may lead to performance losses in the application of a high-speed train passage. This is because the authors attempted to present a more straightforward and practical approach aiming to show the performance of the features proposed without further adjustment or pre-processing.

Table 5. Wheelset fault detection accuracies for measured and boosted data from acoustic M1-M2 sensors

Classifier	Classification Performance (%)				
	WPE	TDF	LCP-K	Sensors	Dataset
FLDA	62.5	56.3	62.5	M1-M2	A2 (4-fold)
	82.0	**93.0**	87.5		SA2 (8-fold)
SVM-I	68.8	62.5	81.3	M1-M2	A2 (4-fold)
	82.8	85.9	**93.0**		SA2 (8-fold)
Dec. Tree	**87.5**	68.8	**87.5**	M1-M2	A2 (4-fold)
	87.5	85.2	87.5		SA2 (8-fold)
PERLC	68.8	75.0	81.3	M1-M2	A2 (4-fold)
	76.6	89.8	89.9		SA2 (8-fold)

5. CONCLUSIONS

Wayside systems for monitoring rail vehicle conditions offer more benefits compared to scheduled maintenance or condition-based repairs (when a fault inevitably appears), particularly in terms of safety and cost-effectiveness. This study focuses on collecting vibration and acoustic signals from the Prague metro tunnel during regular metro operations to establish an effective framework for monitoring the metro wheelset condition. By employing the proposed methods, a precise procedure for detecting wheelset faults is developed.

Initially, vibration sensor data is utilized to identify wheel defects known to exist on the ID-108 metro train set. This is achieved through the application of TDF, WPE, and LCP-K algorithms, coupled with advanced classifiers like SVM-I, Dec. Tree, and PERLC, following speed-adaptive segmentation. Subsequently, ADASYN is employed to ensure the reliability and alignment of measured faulty signals with healthy ones. The results reveal that the two-class problem is addressed with 100% accuracy for both the A1 and SA1 datasets using TDF features and the Dec. Tree classifier.

In addition, the vibration signal dataset is split into two parts,

and a two-class classification is conducted using classifier combination techniques. The results indicate that WPE performs exceptionally well when combined with Med-C, Mean-C, and Vote-C, achieving a 100% success rate in classifying the A1 dataset. However, TDF continues to perform remarkably in classifying the SA1 dataset, achieving an accuracy of 96.1% while LCP-K outperforms WPE in this scenario.

In conclusion, the acoustic signal database is used to assess faulty wheelsets compared to the vibration-based system. While LCP-K shows superior classification accuracy in both measured (A2) and synthesized (SA2) databases (87.5% and 93% respectively), overall accuracy is notably lower in acoustic-based monitoring.

Hence, the methodologies proposed in this study offer the potential to develop suitable frameworks for both acoustic and vibration-based condition monitoring systems, offering simplicity and cost-effectiveness.

The efficiency and applicability of the proposed framework are limited to the complexity of the number of interactions of the rotating device and speed (e.g.: high speed-trains) which can require increased number of wavelet scales or levels in the Kurtogram calculation to prevent low resolution. As a future work, after having adjusted the parameters of the proposed methods to the model-based natural behaviour of the problem in railways, this framework has the potential to assist maintenance specialists and can be adapted for the use of various railway vehicles.

6. METHODOLOGY HIGHLIGHTS

The proposed wayside condition monitoring comprehensive framework includes the following contributions: Model-based one-period analysis for rotating machinery condition monitoring ensures computational efficiency and speed adaptivity. Utilizing ADASYN to address the problem of having a rare number of faulty samples in real-world scenarios helps to balance the datasets. Remarkable recognition accuracies of up to 100% in vibration-based methodologies and up to 93% in acoustic-based methodologies, achieved through leveraging known techniques (WPE and TDF) and the novel LCP-K algorithm, which also address sample length variation problems due to speed fluctuations. The superiority of LCP-K demonstrated in fault detection accuracy, especially in acoustic databases, by employing combined classifier and ADASYN. The presented machine learning scheme is also advantageous over deep learning systems due to the necessity of low number samples and better explanation of the problem.

ACKNOWLEDGMENT

This study was supported by the Competence Centre of Railway Vehicles (TAČR TE01020038), and we are grateful to the Prague Public Transport Company, a.s. for facilitating the measurements.

REFERENCES

[1] Abood, A.M., Nasser, A.R., Al-Khazraji, H. (2022). Predictive maintenance of electromechanical systems using deep learning algorithms. Ingénierie des Systèmes d'Information, 27(6): 1009-1017. https://doi.org/10.18280/isi.270618

[2] Ward, C.P., Goodall, R.M., Dixon, R., Charles, G. (2010). Condition monitoring of rail vehicle bogies. In UKACC International Conference on Control 2010, Coventry, IET, pp. 1-6. https://doi.org/10.1049/ic.2010.0447

[3] Kilinc, O., Vagner, J. (2017). Wayside diagnosis of metro wheelsets using acoustic sensor data and one-period analysis. In Proceedings of the 23rd International Conference Engineering Mechanics, pp. 458-461.

[4] Zakharov, S.M., Zharov, I.A. (2005). Criteria of bogie performance and wheel/rail wear prediction based on wayside measurements. Wear, 258(7-8): 1135-1141. https://doi.org/10.1016/j.wear.2004.03.025

[5] Jakimovska, K., Vasilev, V., Stoimenov, N., Gyoshev, S., Karastoyanov, D. (2015). Train control system for railway vehicles running at operational speed. Manufacturing Engineering, 69(2): 86-92.

[6] Brickle, B., Morgan, R., Smith, E., Brosseau, J., Pinney, C. (2008). Identification of existing and new technologies for wheelset condition monitoring. Transportation Technology Center, United Kingdom, RSSB Report T607 UK P-07-005. https://www.rssb.co.uk/en/research-catalogue/CatalogueItem/rp000304

[7] Alemi, A., Corman, F., Lodewijks, G. (2017). Condition monitoring approaches for the detection of railway wheel defects. Proceedings of the Institution of Mechanical Engineers, Part F: Journal of Rail and Rapid Transit, 231(8): 961-981. https://doi.org/10.1177/0954409716656218

[8] Stratman, B., Liu, Y., Mahadevan, S. (2007). Structural health monitoring of railroad wheels using wheel impact load detectors. Journal of Failure Analysis and Prevention, 7: 218-225. https://doi.org/10.1007/s11668-007-9043-3

[9] Buggy, S.J., James, S.W., Staines, S., Carroll, R., Kitson, P., Farrington, D., Drewett, L., Jaiswal, J., Tatam, R.P. (2016). Railway track component condition monitoring using optical fibre Bragg grating sensors. Measurement Science and Technology, 27(5): 055201. https://doi.org/10.1088/0957-0233/27/5/055201

[10] Filograno, M.L., Guillén, P.C., Rodríguez-Barrios, A., Martín-López, S., Rodríguez-Plaza, M., Andrés-Alguacil, Á., González-Herráez, M. (2011). Real-time monitoring of railway traffic using fiber Bragg grating sensors. IEEE Sensors Journal, 12(1): 85-92. https://doi.org/10.1109/JSEN.2011.2135848

[11] Wei, C., Xin, Q., Chung, W.H., Liu, S.Y., Tam, H.Y., Ho, S.L. (2011). Real-time train wheel condition monitoring by fiber Bragg grating sensors. International Journal of Distributed Sensor Networks, 8(1): 409048. https://doi.org/10.1155/2012/409048

[12] Filograno, M.L., Corredera, P., Rodriguez-Plaza, M., Andres-Alguacil, A., Gonzalez-Herraez, M. (2013). Wheel flat detection in high-speed railway systems using fiber Bragg gratings. IEEE Sensors Journal, 13(12): 4808-4816. https://doi.org/10.1109/JSEN.2013.2274008

[13] Liu, X.Z., Xu, C., Ni, Y.Q. (2019). Wayside detection of wheel minor defects in high-speed trains by a Bayesian blind source separation method. Sensors, 19(18): 3981. https://doi.org/10.3390/s19183981

[14] Palo, M., Galar, D., Nordmark, T., Asplund, M., Larsson, D. (2014). Condition monitoring at the wheel/rail

interface for decision-making support. Proceedings of the Institution of Mechanical Engineers, Part F: Journal of Rail and Rapid Transit, 228(6): 705-715. https://doi.org/10.1177/0954409714526164
[15] Ngigi, R.W., Pislaru, C., Ball, A., Gu, F. (2012). Modern techniques for condition monitoring of railway vehicle dynamics. In Journal of Physics: Conference Series, IOP Publishing, 364(1): 012016. https://doi.org/10.1088/1742-6596/364/1/012016
[16] Yang, K., Ma, L., Gao, X., Wang, L. (2012). Profile parameters of wheelset detection for high speed freight train. In Fourth International Conference on Digital Image Processing (ICDIP 2012), SPIE, 8334: 382-387. https://doi.org/10.1117/12.952474
[17] Brizuela, J., Ibañez, A., Nevado, P., Fritsch, C. (2010). Railway wheels flat detector using Doppler effect. Physics Procedia, 3(1): 811-817. https://doi.org/10.1016/j.phpro.2010.01.104
[18] Brizuela, J., Fritsch, C., Ibáñez, A. (2011). Railway wheel-flat detection and measurement by ultrasound. Transportation Research Part C: Emerging Technologies, 19(6): 975-984. https://doi.org/10.1016/j.trc.2011.04.004
[19] Kenderian, S.H.A.N.T., Djordjevic, B.B., Cerniglia, D., Garcia, G. (2006). Dynamic railroad inspection using the laser-air hybrid ultrasonic technique. Insight-Non-Destructive Testing and Condition Monitoring, 48(6): 336-341. https://doi.org/10.1784/insi.2006.48.6.336
[20] Salzburger, H.J., Schuppmann, M., Li, W., Xiaorong, G. (2009). In-motion ultrasonic testing of the tread of high-speed railway wheels using the inspection system AUROPA III. Insight-Non-Destructive Testing and Condition Monitoring, 51(7): 370-372. https://doi.org/10.1784/insi.2009.51.7.370
[21] Zhong, Z.M., Chen, J., Zhong, P., Wu, J.B. (2006). Application of the blind source separation method to feature extraction of machine sound signals. The International Journal of Advanced Manufacturing Technology, 28: 855-862. https://doi.org/10.1007/s00170-004-2353-7
[22] Li, W., Mechefske, C.K. (2006). Detection of induction motor faults: A comparison of stator current, vibration and acoustic methods. Journal of Vibration and Control, 12(2): 165-188. https://doi.org/10.1177/1077546306062097
[23] Yang, J., Zhang, Y., Zhu, Y. (2007). Intelligent fault diagnosis of rolling element bearing based on SVMs and fractal dimension. Mechanical Systems and Signal Processing, 21(5): 2012-2024. https://doi.org/10.1016/j.ymssp.2006.10.005
[24] Wu, J.D., Liu, C.H. (2009). An expert system for fault diagnosis in internal combustion engines using wavelet packet transform and neural network. Expert Systems with Applications, 36(3): 4278-4286. https://doi.org/10.1016/j.eswa.2008.03.008
[25] Li, W., Tsai, Y.P., Chiu, C.L. (2004). The experimental study of the expert system for diagnosing unbalances by ANN and acoustic signals. Journal of Sound and Vibration, 272(1-2): 69-83. https://doi.org/10.1016/S0022-460X(03)00317-1
[26] Bollas, K., Papasalouros, D., Kourousis, D., Anastasopoulos, A. (2013). Acoustic emission monitoring of wheel sets on moving trains. Construction and Building Materials, 48: 1266-1272. https://doi.org/10.1016/j.conbuildmat.2013.02.013
[27] Devi, S., Kumar, L.S., Shanker, N.R., Prabakaran, K. (2010). A comparative study between vibration and acoustic signals in HTC cooling pump and chilling pump. International Journal of Engineering and Technology, 2(3): 273-277. https://doi.org/10.7763/IJET.2010.V2.133
[28] Liu, Y., Qian, Q., Liu, F., Lu, S., Fu, Y. (2017). Wayside acoustic fault diagnosis of train wheel bearing based on Doppler effect correction and fault-relevant information enhancement. Advances in Mechanical Engineering, 9(11): 1687814017732676. https://doi.org/10.1177/1687814017732676
[29] Bracciali, A., Cascini, G. (1997). Detection of corrugation and wheelflats of railway wheels using energy and cepstrum analysis of rail acceleration. Proceedings of the Institution of Mechanical Engineers, Part F: Journal of Rail and Rapid Transit, 211(2): 109-116. https://doi.org/10.1243/0954409971530950
[30] Skarlatos, D., Karakasis, K., Trochidis, A. (2004). Railway wheel fault diagnosis using a fuzzy-logic method. Applied Acoustics, 65(10): 951-966. https://doi.org/10.1016/j.apacoust.2004.04.003
[31] Belotti, V., Crenna, F., Michelini, R.C., Rossi, G.B. (2006). Wheel-flat diagnostic tool via wavelet transform. Mechanical Systems and Signal Processing, 20(8): 1953-1966. https://doi.org/10.1016/j.ymssp.2005.12.012
[32] Lee, M.L., Chiu, W.K. (2007). Determination of railway vertical wheel impact magnitudes: Field trials. Structural Health Monitoring, 6(1): 49-65. https://doi.org/10.1177/1475921707072063
[33] Mao, C., Jiang, Y., Wang, D., Chen, X., Tao, J. (2015). Modeling and simulation of non-stationary vehicle vibration signals based on Hilbert spectrum. Mechanical Systems and Signal Processing, 50: 56-69. https://doi.org/10.1016/j.ymssp.2014.05.005
[34] Hloušek, P. (2008). Phase analysis of interference currents of railway vehicles. Electroscope, Applied Electronics, 2008(3): 241-244.
[35] Mohammadi, M., Mosleh, A., Vale, C., Ribeiro, D., Montenegro, P., Meixedo, A. (2023). An unsupervised learning approach for wayside train wheel flat detection. Sensors, 23(4): 1910. https://doi.org/10.3390/s23041910
[36] Wang, W., Wong, A.K. (2002). Autoregressive model-based gear fault diagnosis. Journal of Vibration and Acoustics, 124(2): 172-179. https://doi.org/10.1115/1.1456905
[37] Wang, F., Mechefske, C.K. (2006). Adaptive modelling of transient vibration signals. Mechanical Systems and Signal Processing, 20(4): 825-842. https://doi.org/10.1016/j.ymssp.2004.12.004
[38] Lei, Y., Zuo, M.J., He, Z., Zi, Y. (2010). A multidimensional hybrid intelligent method for gear fault diagnosis. Expert Systems with Applications, 37(2): 1419-1430. https://doi.org/10.1016/j.eswa.2009.06.060
[39] Sreejith, B., Verma, A.K., Srividya, A. (2008). Fault diagnosis of rolling element bearing using time-domain features and neural networks. In 2008 IEEE Region 10 and The Third International Conference on Industrial and Information Systems, Kharagpur, India, pp. 1-6. https://doi.org/10.1109/ICIINFS.2008.4798444
[40] Pan, Y., Chen, J., Guo, L. (2009). Robust bearing performance degradation assessment method based on improved wavelet packet-support vector data description.

Mechanical Systems and Signal Processing, 23(3): 669-681. https://doi.org/10.1016/j.ymssp.2008.05.011
[41] Kankar, P.K., Sharma, S.C., Harsha, S.P. (2011). Fault diagnosis of ball bearings using machine learning methods. Expert Systems with Applications, 38(3): 1876-1886. https://doi.org/10.1016/j.eswa.2010.07.119
[42] Aherwar, A. (2012). An investigation on gearbox fault detection using vibration analysis techniques: A review. Australian Journal of Mechanical Engineering, 10(2): 169-183. https://doi.org/10.7158/M11-830.2012.10.2
[43] Belaid, K., Miloudi, A. (2013). Detection of gear defects by resonance demodulation detected by wavelet transform and comparison with the kurtogram. 21st French Mechanical Congress, Bordeaux, France, pp. 1-6.
[44] Li, P., Kong, F., He, Q., Liu, Y. (2013). Multiscale slope feature extraction for rotating machinery fault diagnosis using wavelet analysis. Measurement, 46(1): 497-505. https://doi.org/10.1016/j.measurement.2012.08.007
[45] McDonald, G.L., Zhao, Q., Zuo, M.J. (2012). Maximum correlated Kurtosis deconvolution and application on gear tooth chip fault detection. Mechanical Systems and Signal Processing, 33: 237-255. https://doi.org/10.1016/j.ymssp.2012.06.010
[46] Yan, R., Gao, R.X., Chen, X. (2014). Wavelets for fault diagnosis of rotary machines: A review with applications. Signal Processing, 96: 1-15. https://doi.org/10.1016/j.sigpro.2013.04.015
[47] Yu, X., Ding, E., Chen, C., Liu, X., Li, L. (2015). A novel characteristic frequency bands extraction method for automatic bearing fault diagnosis based on Hilbert Huang transform. Sensors, 15(11): 27869-27893. https://doi.org/10.3390/s151127869
[48] Fu, S., Liu, K., Xu, Y., Liu, Y. (2016). Rolling bearing diagnosing method based on time domain analysis and adaptive fuzzy-means clustering. Shock and Vibration, 2016. https://doi.org/10.1155/2016/9412787
[49] Antoni, J. (2007). Fast computation of the kurtogram for the detection of transient faults. Mechanical Systems and Signal Processing, 21(1): 108-124. https://doi.org/10.1016/j.ymssp.2005.12.002
[50] Wang, M., Hu, N.Q., Hu, L., Gao, M. (2013). Feature optimization for bearing fault diagnosis. In 2013 International Conference on Quality, Reliability, Risk, Maintenance, and Safety Engineering (QR2MSE), Chengdu, China, IEEE, pp. 1738-1741. https://doi.org/10.1109/QR2MSE.2013.6625912
[51] Toh, G., Park, J. (2020). Review of vibration-based structural health monitoring using deep learning. Applied Sciences, 10(5): 1680. https://doi.org/10.3390/app10051680
[52] Shaikh, K., Hussain, I., Chowdhry, B.S. (2023). Wheel defect detection using a hybrid deep learning approach. Sensors, 23(14): 6248. https://doi.org/10.3390/s23146248
[53] Fu, W., He, Q., Feng, Q., Li, J., Zheng, F., Zhang, B. (2023). Recent advances in wayside railway wheel flat detection techniques: A review. Sensors, 23(8): 3916. https://doi.org/10.3390/s23083916
[54] Lourenço, A., Ferraz, C., Ribeiro, D., Mosleh, A., Montenegro, P., Vale, C., Meixedo, A., Marreiros, G. (2023). Adaptive time series representation for out-of-round railway wheels fault diagnosis in wayside monitoring. Engineering Failure Analysis, 152: 107433. https://doi.org/10.1016/j.engfailanal.2023.107433
[55] Ngamkhanong, C., Kaewunruen, S., Costa, B.J.A. (2018). State-of-the-art review of railway track resilience monitoring. Infrastructures, 3(1): 3. https://doi.org/10.3390/infrastructures3010003
[56] Komorski, P., Szymanski, G.M., Nowakowski, T., Orczyk, M. (2021). Advanced acoustic signal analysis used for wheel-flat detection. Latin American Journal of Solids and Structures, 18: e338. https://doi.org/10.1590/1679-78256086
[57] Rioul, O., Vetterli, M. (1991). Wavelets and signal processing. IEEE Signal Processing Magazine, 8(4): 14-38. https://doi.org/10.1109/79.91217
[58] Chabchoub, S., Mansouri, S., Salah, R.B. (2016). Impedance cardiography signal denoising using discrete wavelet transform. Australasian Physical & Engineering Sciences in Medicine, 39: 655-663. https://doi.org/10.1007/s13246-016-0460-z
[59] Addison, P.S. (2005). Wavelet transforms and the ECG: A review. Physiological Measurement, 26(5): R155. https://doi.org/10.1088/0967-3334/26/5/R01
[60] Akansu, A.N., Haddad, R.A. (2001). Multiresolution Signal Decomposition: Transforms, Subbands, and Wavelets. Academic Press. 2nd ed. San Diego: Academic Press.
[61] Yen, G.G., Lin, K.C. (2000). Wavelet packet feature extraction for vibration monitoring. IEEE Transactions on Industrial Electronics, 47(3): 650-667. https://doi.org/10.1109/41.847906
[62] Yen, G.G., Lin, K.C. (2000). Wavelet packet feature extraction for vibration monitoring. IEEE Transactions on Industrial Electronics, 47(3): 650-667. https://doi.org/10.1109/41.847906
[63] Dwyer, R. (1983). Detection of non-Gaussian signals by frequency domain kurtosis estimation. In ICASSP'83. IEEE International Conference on Acoustics, Speech, and Signal Processing, Boston, MA, USA, 8: 607-610. https://doi.org/10.1109/ICASSP.1983.1172264
[64] Zhou, S.R., Yin, J.P., Zhang, J.M. (2013). Local binary pattern (LBP) and local phase quantization (LBQ) based on Gabor filter for face representation. Neurocomputing, 116: 260-264. https://doi.org/10.1016/j.neucom.2012.05.036
[65] Ergin, S., Kilinç, O. (2013). Using DSIFT and LCP features for detecting breast lesions. In International Symposium on Computing in Science & Engineering. Proceedings. GEDIZ University, Engineering and Architecture Faculty, p. 216-220.
[66] Guo, Y., Zhao, G., Pietikäinen, M. (2011). Texture classification using a linear configuration model based descriptor. In Proceedings of the British Machine Vision Conference, pp. 1-10.
[67] Zeng, L., Li, X., Xu, J. (2013). An improved joint dictionary training method for single image super resolution. COMPEL-The International Journal for Computation and Mathematics in Electrical and Electronic Engineering, 32(2): 721-727. https://doi.org/10.1108/03321641311297142
[68] Kilinc, O., Vágner, J. (2017). Detecting anomalous sensor data in wayside diagnostics using enhanced LBP-kurtograms. Perner's Contacts, 12(4): 23-30.
[69] Koç, M., Barkana, A., Gerek, Ö.N. (2010). A fast method for the implementation of common vector approach. Information Sciences, 180(20): 4084-4098. https://doi.org/10.1016/j.ins.2010.06.027

[70] Chawla, N.V., Bowyer, K.W., Hall, L.O., Kegelmeyer, W.P. (2002). SMOTE: Synthetic minority over-sampling technique. Journal of Artificial Intelligence Research, 16: 321-357. https://doi.org/10.1613/jair.953
[71] He, H., Bai, Y., Garcia, E.A., Li, S. (2008). ADASYN: Adaptive synthetic sampling approach for imbalanced learning. In 2008 IEEE International Joint Conference on Neural Networks (IEEE World Congress on Computational Intelligence), Hong Kong, pp. 1322-1328. https://doi.org/10.1109/IJCNN.2008.4633969
[72] Kilinc, O. (2017). Wayside diagnosis of running gear related faults in railway vehicles. Doctoral Thesis, University of Pardubice, Czechia.
[73] Kim, J., Kim, B.S., Savarese, S. (2012). Comparing image classification methods: K-nearest-neighbor and support-vector-machines. In Proceedings of the 6th WSEAS International Conference on Computer Engineering and Applications, and Proceedings of the 2012 American Conference on Applied Mathematics, pp. 133-138.
[74] Sholahuddin, A., Ramadhan, A.P., Supriatna, A.K. (2015). The application of ANN-Linear Perceptron in the development of DSS for a fishery industry. Procedia Computer Science, 72: 67-77. https://doi.org/10.1016/j.procs.2015.12.106
[75] Loog, M., Duin, R.P.W., Haeb-Umbach, R. (2001). Multiclass linear dimension reduction by weighted pairwise Fisher criteria. IEEE Transactions on Pattern Analysis and Machine Intelligence, 23(7): 762-766. https://doi.org/10.1109/34.935849
[76] Safavian, S.R., Landgrebe, D. (1991). A survey of decision tree classifier methodology. IEEE Transactions on Systems, Man, and Cybernetics, 21(3): 660-674. https://doi.org/10.1109/21.97458
[77] Duin, R.P. (2002). The combining classifier: To train or not to train?. In 2002 International Conference on Pattern Recognition, Quebec City, QC, Canada, 2: 765-770. https://doi.org/10.1109/ICPR.2002.1048415

NOMENCLATURE

f_{ws}	rotating frequency of the wheelset, s^{-1}
v	translational velocity of the train, $m.s^{-1}$
D_k	wheel diameter on k-th index, mm
n_i	number of samples in the block
d_i	mean diameter of right and left wheels, mm
f_s	sampling frequency of the recorded signals, s^{-1}
L	distance between optical gates, m
s_{Ai}	sample number of detecting centre for *OGA*
s_{Bi}	sample number of detecting centre for *OGB*
$x[n]$	sample discrete signal
n_w	number of levels (scales) in wavelet transform
k_w	number of packets in wavelet transform
$h[n]$	low-pass filter in wavelet transform
$g[n]$	high-pass filter in wavelet transform
$c_{j,n}$	wavelet coefficients in wavelet transform
n_o	size of feature vector in each class
E_{n_w,k_w}	wavelet packet energy in w-th packet
g_c	centre pixel intensity in LBP
m_o	number observations in each class
m_0^{Faulty}	number observations in faulty class
m_0^{Normal}	number observations in normal class

Greek symbols

ψ	wavelet basis function
μ	mean value in TDF
σ	standard deviation value in TDF

Subscripts

a, b	dilation, location parameters for wavelet function
R	circular radius in LBP algorithm
N	number of samples in the signal sample